Am J Transl Res 2024;16(1):27-38
www.ajtr.org /ISSN:1943-8141/AJTR0153267

Original Article

Artemether regulates liver glycogen and lipid utilization through mitochondrial pyruvate oxidation in db/db mice

Wenci Weng[1*], Lingling Shen[4*], Xuewen Yu[2], Rui Yuan[3], Mumin Shao[2], Pengxun Han[1], Huili Sun[4]

[1]Department of Nephrology, Shenzhen Traditional Chinese Medicine Hospital, The Fourth Clinical Medical College of Guangzhou University of Chinese Medicine, No. 1 Fuhua Road, Futian District, Shenzhen 518033, Guangdong, China; [2]Department of Pathology, Shenzhen Traditional Chinese Medicine Hospital, The Fourth Clinical Medical College of Guangzhou University of Chinese Medicine, No. 1 Fuhua Road, Futian District, Shenzhen 518033, Guangdong, China; [3]Department of Clinical Laboratory, Shenzhen Traditional Chinese Medicine Hospital, The Fourth Clinical Medical College of Guangzhou University of Chinese Medicine, No. 1 Fuhua Road, Futian District, Shenzhen 518033, Guangdong, China; [4]Department of Nephrology, Shenzhen Traditional Chinese Medicine Hospital Affiliated to Nanjing University of Chinese Medicine, No. 1 Fuhua Road, Futian District, Shenzhen 518033, Guangdong, China. [*]Equal contributors.

Received September 3, 2023; Accepted December 29, 2023; Epub January 15, 2024; Published January 30, 2024

Abstract: Objectives: Diabetes is an important global health problem. The occurrence and development of type 2 diabetes (T2D) involves multiple organs, among which the liver is an important organ. Artemether is a methyl ether derivative of artemisinin and has displayed significant antidiabetic effects. However, its regulation of glucose metabolism is not clearly elucidated. This study explored the effect of artemether on liver mitochondrial pyruvate metabolism. Methods: T2D db/db mice were used and grouped into db/db and db/db+Art groups. Lean wild type mice served as control. After artemether intervention for 12 weeks, the respiratory exchange ratio (RER), redox state, relevant serum lipid content, liver glycogen and lipid content, liver insulin and insulin-like growth factor 1 (IGF-1) signal transduction, mitochondrial pyruvate oxidation pathway, fatty acid and glycogen metabolic pathways were evaluated. Results: This experiment demonstrated that artemether raised RER and enhanced liver mitochondrial pyruvate metabolism in db/db mice. Artemether also reduced serum and urinary lipid peroxidation products and regulated the redox status in liver. The accumulation of liver glycogen in diabetic mice was attenuated, the proportion of lipid content in serum and liver was changed by artemether. The signal pathway associated with liver glycogen metabolism was also regulated by artemether. In addition, artemether increased serum insulin and regulated insulin/IGF-1 signal pathway in liver. Conclusions: The present study confirmed that artemether can regulate liver glycogen and lipid utilization in T2D mice, its biological mechanisms were associated with mitochondrial pyruvate oxidation in the liver.

Keywords: Artemether, liver, glycogen, lipid, pyruvate

Introduction

Diabetes is an important global health problem. Although many studies have tried to elucidate its pathogenesis, the pathophysiological process remains elusive. Type 2 diabetes (T2D) accounts for the majority of cases of diabetes and primarily occurs as a result of overnutrition [1]. The occurrence and development of T2D involves multiple organs, among which the liver is an important organ [2].

As the main site of carbohydrate and lipid metabolism, the liver plays a major role in the regulation of blood glucose homeostasis [3]. Under a normal physiological state, the liver synthesizes and stores glycogen via glycogenesis when the body has excess blood glucose. When needed, it releases glucose into the blood via glycogenolysis (the breakdown of glycogen into glucose) and gluconeogenesis (the generation of glucose from certain non-carbohydrate substrates) [4]. The liver also performs anabolism and catabolism of fatty acid, triglycerides, cholesterol and lipoprotein [5]. In prediabetes, such as obesity, disordered glycogen and lipid utilization occur in the liver and are deeply involved in the initiation of diabetes [2].

https://doi.org/10.62347/NEAS4467

The glucose fatty-acid cycle (Randle cycle) is a metabolic process and it refers to the competition of glucose and fatty acids for substrates. Many studies have indicated that this biological process partly explains the causes of diabetes [6]. In a diabetic state, the body presents lower respiratory exchange ratio (RER) which indicates that lipids are the predominant fuel source of energy [7, 8]. Some researchers hold the opinion that fatty acid oxidation would give higher reactive oxygen species (ROS) formation than glucose oxidation [9-11]. Our previous studies also support this viewpoint [12]. However, the detailed mechanism still needs further exploration. As the main site of cellular pyruvate and fatty acid oxidation, mitochondria play a key role in the selection of energy substrates [13, 14]. The liver is an organ with abundant mitochondria and pyruvate is the key hub bridging glucose and lipid metabolism. Therefore, we speculated that liver mitochondrial pyruvate metabolism might be an important therapeutic target for T2D.

Artemether is a methyl ether derivative of artemisinin and is widely used for malaria therapy [15]. Its biological mechanism was associated with regulating mitochondrial function and redox state [12, 16, 17]. Some studies have shown that it also displayed significant antidiabetic effect [18]. However, its regulation on glucose metabolism was not clearly elucidated. Here, we performed this experiment to explore the effect of artemether on liver mitochondrial pyruvate metabolism.

Materials and methods

Animal experiments

Animal experiments were approved and performed according to relevant guidelines and regulations of The Institutional Animal Care and Use Committee at Guangzhou University of Chinese Medicine. Male db/db mice (BKS.Cg-Dock7$^{m+/+}$Lepr^{db}/Nju) and lean wild type control mice were obtained from the Model Animal Research Center of Nanjing University. The 8-week-old db/db mice were randomly divided into the db/db group and db/db+artemether (db/db+Art) group. Age-matched lean wild type mice served as normal control group mice. The control and db/db group mice were fed a regular standard diet. The db/db+Art group mice were fed a medicated diet containing 0.67 g/kg artemether (Chengdu ConBon Bio-tech Co., Ltd.). The intervention time lasted for 12 weeks.

Tissue preparation

After intervention, the mice were sacrificed before blood collection. The liver tissues were then isolated and weighed. Partial liver tissue was fixed in 10% formalin for histopathological examination and immunohistochemical staining. The remaining tissues were immediately frozen in liquid nitrogen and stored at -80°C for future analysis.

Physiological metabolism monitoring and biochemical determination

At the end of the experiment, RER was determined using the Comprehensive Lab Animal Monitoring System (Columbus Instruments, Columbus, OH, USA). The urine of each group was collected using metabolic cages (Tecniplast, Buguggiate, Italy). Serum triglyceride (TG) and total cholesterol (TC) were measured by using an automatic biochemical analyzer (Roche, Basel, Switzerland). Serum malondialdehyde (MDA) was measured according to the kit instruction (cat. no. A003-1, Nanjing Jiancheng Bioengineering Institute, Nanjing, China). Liver glycogen content was quantified using the Anthrone method. Liver content of TG, free fatty acid (FFA), TC, glutathione (GSH) and serum level of FFA were determined according to the kit instructions (TG, cat. no. BC0625; FFA, cat. no. BC0595; TC, cat. no. BC1985; GSH, cat. no. BC1175; Beijing Solarbio Science & Technology Co., Ltd., Beijing, China).

Histopathological analysis

Paraffin sections of the liver tissues were stained with periodic acid-Schiff (PAS) and diastase (D)-PAS to display the glycogen content and alterations. Sections were stained with hematoxylin and eosin (HE) to observe the lipid changes in the liver. For each sample, 10-15 images were randomly selected to calculate the lipid droplets area ratio. The sections were scanned using the Digital Slide Scanner (3DHistech Ltd.).

Immunohistochemical staining

Briefly, liver sections were deparaffinized and rehydrated. After antigen retrieval using citrate

buffer, the sections were incubated with primary antibodies against pyruvate dehydrogenase kinase 1 (PDK1; Enzo Life Science; ADI-KAP-PK112-F) and insulin receptor substrate 1 (IRS1; Proteintech; 17509-1-AP) overnight at 4°C. The sections were then washed and incubated with HRP-conjugated secondary antibodies (Fuzhou MaiXin Biotech Co., Ltd.; cat. no. KIT-5020) for 1 h at room temperature. Diaminobenzidine solution was used as chromogenic reagent. The sections were counterstained using hematoxylin and images were acquired by the Digital Slide Scanner.

ELISA

Serum levels of insulin (EMD Millipore; cat. no. #EZRMI-13K), insulin-like growth factor 1 (IGF-1; R&D Systems; cat. no. MG100) and urinary 4-Hydroxynonenal (4HNE; Nanjing Jiancheng Bioengineering Institute; cat. no. H268) and 8-hydroxydeoxyguanosine (8-OHdG; Nanjing Jiancheng Bioengineering Institute; cat. no. H165) were measured according to the ELISA kit instructions.

Immunoblotting analysis

Liver tissues were homogenized and prepared in sample loading buffer (Bio-Rad Laboratories, Inc.). The homogenates were separated on SDS-PAGE gels and transferred to PVDF membranes (MilliporeSigma). After blocking, the membranes were incubated overnight at 4°C with the following primary antibodies: pyruvate dehydrogenase (PDH; CST#2784), p-PDH (Ser293) (CST#31866), PDK1 (Enzo Life Science; ADI-KAP-PK112-F), pyruvate dehydrogenase kinase 4 (PDK4; Proteintech; 12949-1-AP), mitochondrial pyruvate carrier 1 (MPC1; Novus; NBP1-91706), mitochondrial pyruvate carrier 2 (MPC2; Proteintech; 20049-1-AP), superoxide dismutase 1 (SOD1; CST#37385), superoxide dismutase 2 (SOD2; CST#13141), superoxide dismutase 3 (SOD3; Proteintech; 14316-1-AP), Catalase (CST#14097), glutathione peroxidase 1 (GPX1; GTX116040), glutathione peroxidase 4 (GPX4; Proteintech; 67763-1-Ig), carnitine palmitoyltransferase 1A (CPT1A; Proteintech; 15184-1-AP), carnitine palmitoyltransferase 2 (CPT2; Proteintech; 26555-1-AP), carnitine octanoyltransferase (CROT; Proteintech; 13543-1-AP), carnitine acetyltransferase (CRAT; Proteintech; 15170-1-AP), acyl-Coenzyme A dehydrogenase very long chain (ACADVL; Proteintech; 14527-1-AP), acyl-Coenzyme A dehydrogenase long chain (ACADL; Proteintech; 17526-1-AP), acyl-Coenzyme A dehydrogenase medium chain (ACADM; Proteintech; 55210-1-AP), Acyl-Coenzyme A dehydrogenase short chain (ACADS; Proteintech; 16623-1-AP), Glycogen synthase (GS; CST#3886), p-GS (Ser-641) (CST#3891), Glycogen phosphorylase liver form (PYGL; Abcam; ab198268), Phosphoenolpyruvate carboxykinase 1 (PCK1; Proteintech; 16754-1-AP), phosphoenolpyruvate carboxykinase 2 (PCK2; Proteintech; 14892-1-AP), glucose 6-phosphatase (G6Pase; Abcam; ab-83690), IRS1 (Proteintech; 17509-1-AP), insulin receptor substrate 2 (IRS2; Proteintech; 20702-1-AP), Vinculin (CST#13901). Then the membranes were incubated with secondary antibodies and detected using the ChemiDoc Imaging System (Bio-Rad Laboratories, Inc.). Vinculin was used as a loading control.

Statistical analysis

Data are presented as the mean ± standard deviation. One-way analysis of variance followed by least significant difference post hoc test was applied in data analysis by SPSS software (Version 22.0; IBM Corp.). $P<0.05$ was considered to indicate a statistically significant difference.

Results

Artemether raised RER and enhanced liver mitochondrial pyruvate metabolism in db/db mice

RER is an important physiological index used to evaluate substrate utilization [19]. Compared to control group mice, significant reduction of RER was observed in db/db mice (**Figure 1A**, **1B**). In diabetic db/db mice, significantly increased p-PDH and PDK1 were detected (**Figure 1C**, **1D**, **1F**). The protein level of PDK4 was also increased slightly but not to significant degree (**Figure 1C**, **1G**). There were no significant differences of PDH, MPC1, and MPC2 between the control group and db/db group (**Figure 1C**, **1E**, **1H**, **1I**). After artemether treatment, the RER in both dark and light phases was significantly raised (**Figure 1A**, **1B**), the protein levels of p-PDH, PDK1, and PDK4 were significantly reduced (**Figure 1C**, **1D**, **1F**, **1G**), the protein level of MPC1 and MPC2 were obviously increased in varying degrees (**Figure 1C**,

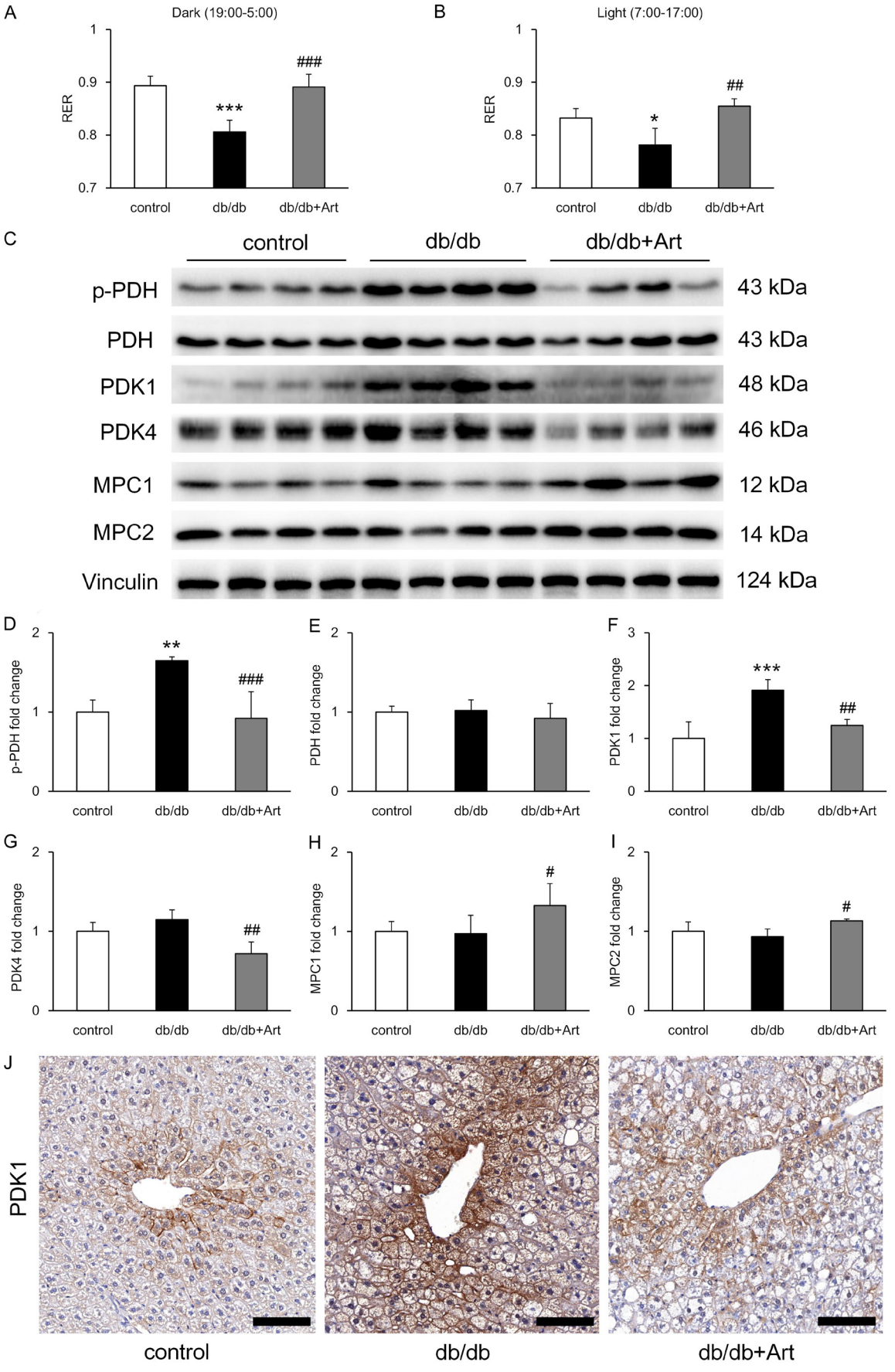
A
Dark (19:00-5:00)
RER
1
0.9
0.8
0.7
***
###
control
db/db
db/db+Art
B
Light (7:00-17:00)
RER
1
0.9
0.8
0.7
*
##
control
db/db
db/db+Art
C
control
db/db
db/db+Art
p-PDH
43 kDa
PDH
43 kDa
PDK1
48 kDa
PDK4
46 kDa
MPC1
12 kDa
MPC2
14 kDa
Vinculin
124 kDa
D
p-PDH fold change
**
###
E
PDH fold change
F
PDK1 fold change
***
##
G
PDK4 fold change
##
H
MPC1 fold change
#
I
MPC2 fold change
#
control
db/db
db/db+Art
J
PDK1
control
db/db
db/db+Art

Figure 1. Effect of artemether on RER and the major proteins involved in pyruvate oxidation in liver. A, B. RER values for the dark and light phase in each group. n=4 per group. C. Immunoblotting bands of p-PDH, PDH, PDK1, PDK4, MPC1, and MPC2 in various groups. D-I. Bar graphs displaying the fold changes of p-PDH, PDH, PDK1, PDK4, MPC1, and MPC2 in different groups. n=4 per group. *P<0.05, **P<0.01 and ***P<0.001 vs. control group; $^{\#}$P<0.05, $^{\#\#}$P<0.01 and $^{\#\#\#}$P<0.001 vs. the db/db group. J. Representative immunohistochemical staining images of PDK1 from each group. Scale bar, 100 μm.

1H, **1I**). The immunohistochemical staining displayed that PDK1 was mainly distributed surrounding the liver central vein and the expression level was in line with the immunoblotting result (**Figure 1J**).

Artemether reduced serum and urinary lipid peroxidation products, regulated the redox status in liver

Compared to control group mice, significantly increased serum level of MDA (**Figure 2A**), and increased urinary excretion of 4HNE and 8-OHdG (**Figure 2B**, **2C**) were measured in db/db mice. Artemether treatment significantly reduced their levels (**Figure 2A-C**). As shown in **Figure 2D**, obviously increased liver content of GSH was determined in db/db mice, but it was not changed by artemether. In diabetic db/db mice, obviously increased GPX4 and unchanged SOD1, SOD2, SOD3, catalase, and GPX1 were observed (**Figure 2E-K**). After artemether intervention, significantly decreased GPX1 and increased SOD1 and GPX4 were detected (**Figure 2E**, **2F**, **2J**, **2K**).

Effects of artemether on metabolic pathway associated with fatty acid oxidation

In db/db mice, significant increased protein levels of CPT1A, CRAT, and ACADM in liver were observed (**Figure 3A**, **3B**, **3E**, **3H**). There were no significant differences of CPT2, CROT, ACADVL, ACADL, and ACADS between control and diabetic group (**Figure 3A**, **3C**, **3D**, **3F**, **3G**, **3I**). Although some protein levels such as CPT1A, CRAT and ACADM were reduced by artemether mildly but not to significant degree (**Figure 3A-I**).

Effects of artemether on signaling pathways related to liver glycogen metabolism

In db/db mice, significantly increased protein levels of p-GS, GS, and PYGL were detected in the liver (**Figure 4A-D**). Meanwhile, a significant reduction of G6Pase content was observed in diabetic liver (**Figure 4A**, **4G**). There were no significant differences of PCK1 and PCK2 between control and diabetic group (**Figure 4A**, **4E**, **4F**). Compared to db/db group mice, p-GS level was significantly increased by artemether (**Figure 4A**, **4B**). The levels of GS, PYGL, PCK1, PCK2, and G6Pase were not changed after artemether treatment (**Figure 4A**, **4C-G**).

Artemether changed the proportion of lipid content in serum and liver

As shown in **Figure 5A-F**, significantly increased serum levels and liver contents of TG, FFA, TC were detected. Consistent with the results of liver biochemical assay, HE staining of liver sections showed that the lipid droplets area ratio in db/db mice was increased significantly compared to control group (**Figure 5G**, **5H**). After artemether treatment, serum levels of TG and FFA were significantly decreased (**Figure 5A**, **5B**), serum TC and liver TG and were significantly increased (**Figure 5C**, **5D**). However, liver content of FFA and TC, and lipid droplet area ratio in the liver were increased slightly by artemether but not to a significant degree (**Figure 5E-H**).

Artemether reduced liver glycogen content in db/db mice

In diabetic db/db mice, abnormally increased liver weight and accumulated liver glycogen were detected (**Figure 6A**, **6B**). After artemether treatment, glycogen content was significantly reduced while the liver weight was not affected (**Figure 6A**, **6B**). Consistent with the results of biochemical determination, the PAS and D-PAS staining displayed the alteration of glycogen in various groups (**Figure 6C**, **6D**).

Artemether regulated insulin and IGF-1 associated pathway in liver

In diabetic db/db mice, significantly increased serum levels of insulin and IGF-1 were measured (**Figure 7A**, **7B**). The liver in db/db mice displayed significantly reduced IRS1 and non-

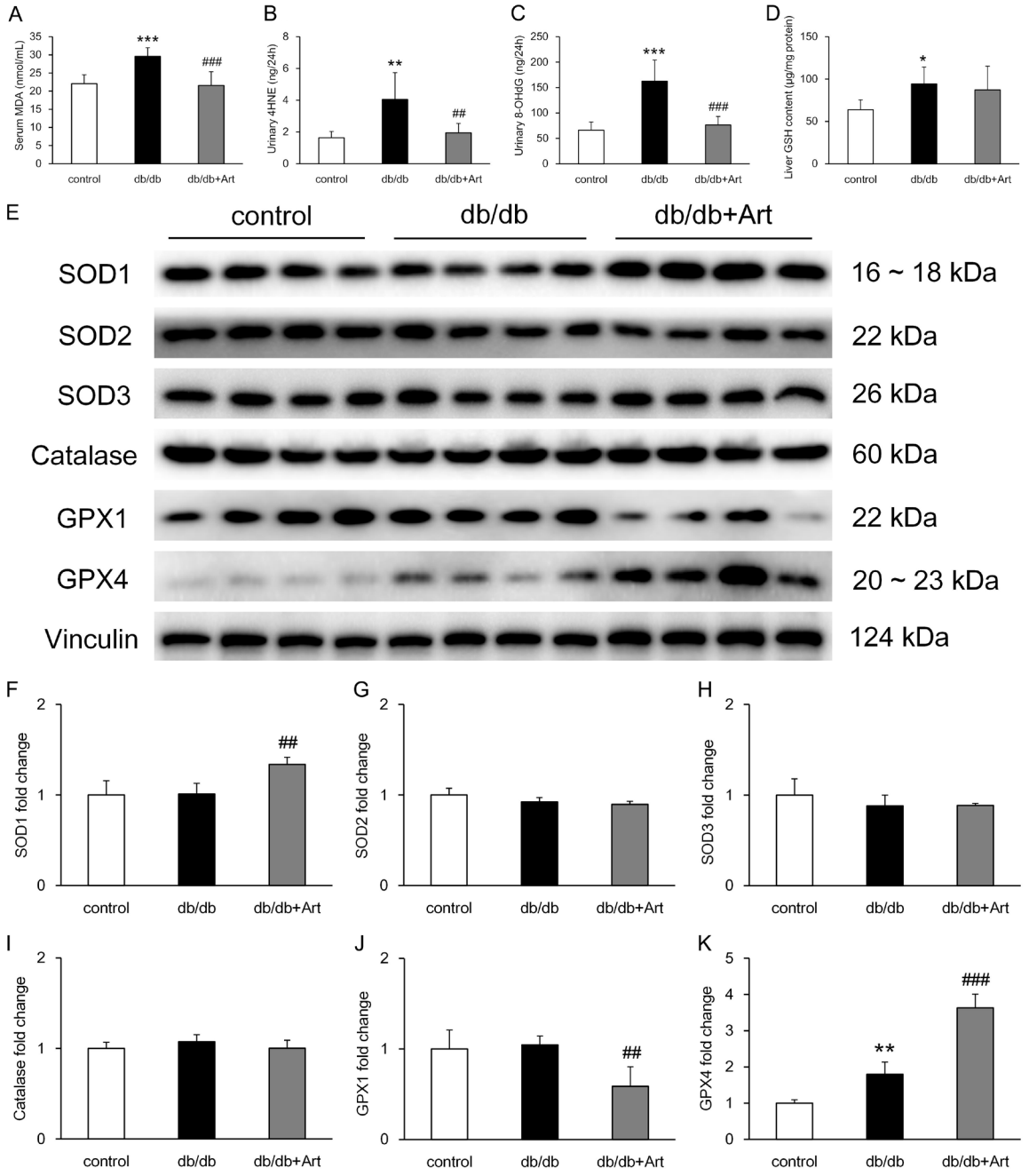

Figure 2. Artemether reduced serum and urinary lipid peroxidation products, regulated the redox status in liver. A. The serum level of MDA in each group. B, C. The urinary 4HNE and 8-OHdG excretion in different groups. D. Bar graph showed the liver GSH content in each group. n=6 per group. E. Immunoblotting bands of SOD1, SOD2, SOD3, Catalase, GPX1, and GPX4 in various groups. F-K. Bar graphs displaying the fold changes of SOD1, SOD2, SOD3, Catalase, GPX1, and GPX4 in different groups. n=4 per group. *P<0.05, **P<0.01 and ***P<0.001 vs. control group; $^{\#\#}$P<0.01 and $^{\#\#\#}$P<0.001 vs. the db/db group.

significant reduction of IRS2 (**Figure 7C-E**). After artemether treatment, serum insulin and liver IRS1 were significantly increased (**Figure 7A**, **7C**, **7D**). The serum IGF-1 and liver IRS2 were not obviously changed by artemether (**Figure 7B**, **7C**, **7E**). The immunohistochemical staining revealed that IRS1 mainly distributed in the hepatic plasma membrane and the expression level was in line with the immunoblotting result (**Figure 7F**).

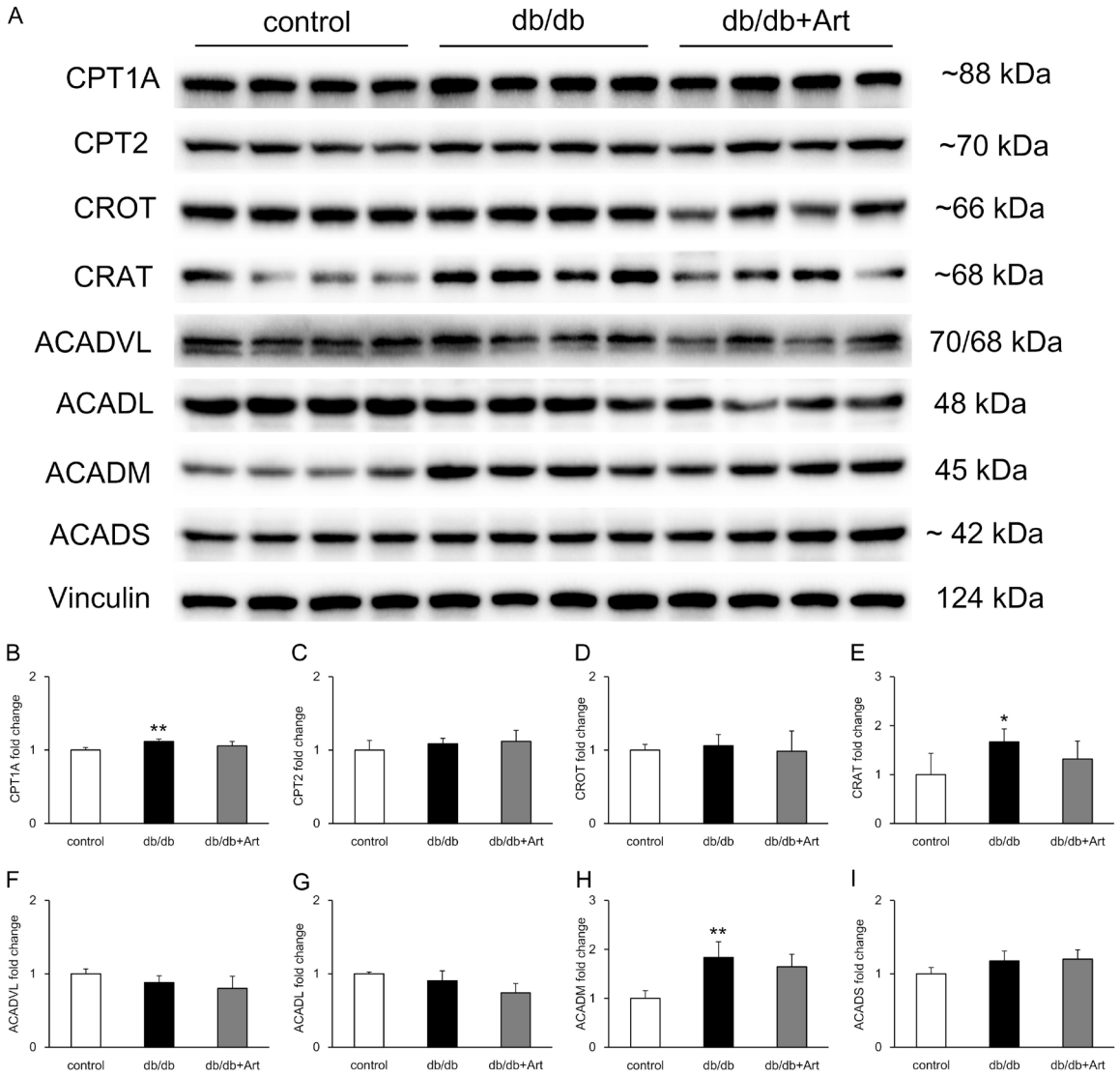

Figure 3. Effects of artemether on fatty acid oxidation in liver. A. Immunoblotting bands of CPT1A, CPT2, CROT, CRAT, ACADVL, ACADL, ACADM, and ACADS in various groups. B-I. Bar graphs displaying the fold changes of CPT1A, CPT2, CROT, CRAT, ACADVL, ACADL, ACADM, and ACADS in different groups. n=4 per group. $^{*}P<0.05$ and $^{**}P<0.01$ vs. control group.

Discussion

In this study, we reported that artemether could enhance liver mitochondrial pyruvate metabolism in T2D. This biological effect may partly explain its regulatory role in liver glycogen and lipid utilization.

In db/db mice, lower RER state, increased serum MDA, and increased urinary 4HNE and 8-OHdG excretion all suggested that fatty acid oxidation was the main energy source of the diabetic mice. From the randle cycle perspective, glucose oxidation and fatty acid oxidation are competitively inhibited mutually in diabetes [6]. In liver tissue of db/db mice, significantly increased p-PDH and PDK1 suggested that mitochondrial pyruvate oxidation was suppressed. Considering that the liver is an important organ of energy metabolism, we inferred that lower RER value in diabetic mice was partly caused by fatty acid utilization in liver. Artemether treatment relieved the suppression of PDKs on pyruvate oxidation and increased pyruvate transporters in the mitochondrial inner membrane. The liver is an organ rich in mitochondria and serves as a hub for various key metabolic pathways [20]. The reinforcement of artemether on liver mitochondrial pyruvate oxidation may contribute to its elevating effect on RER.

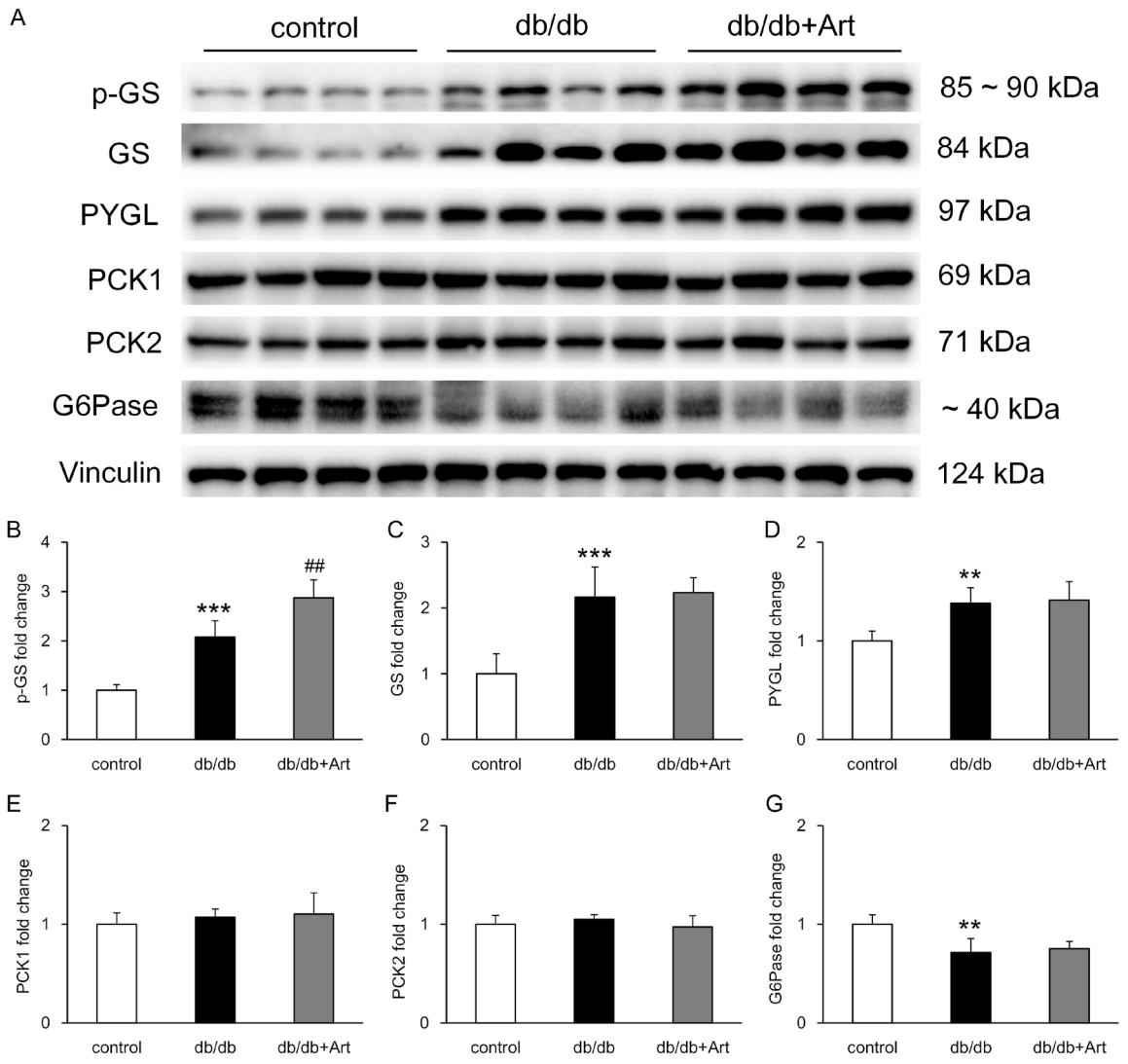

Figure 4. Artemether regulated signaling pathways associated with glycogen metabolism. A. Immunoblotting bands of p-GS, GS, PYGL, PCK1, PCK2, and G6Pase in various groups. B-G. Bar graphs displaying the fold changes of p-GS, GS, PYGL, PCK1, PCK2, and G6Pase in different groups. n=4 per group. $^{**}P<0.01$ and $^{***}P<0.001$ vs. control group; $^{\#\#}P<0.01$ vs. the db/db group.

Lipid metabolism disorder is a typical feature of diabetes. In db/db mice, pathological changes and biochemical tests indicated that excessive lipid deposition in the liver. Artemether treatment displayed a promoting effect on lipid accumulation in the liver. Serum TC was also increased after artemether treatment. Interestingly, both serum TG and FFA were significantly reduced by artemether. Therefore, we speculate that artemether may be involved in the transport of lipids between the blood circulation and the liver, and has a certain regulatory effect on hepatic lipid synthesis. In addition, significantly enhanced β-oxidation of the medium-chain fatty acids in the liver were observed in db/db mice. Accompanied by fatty acid oxidation, higher ROS were produced [10]. The present study also supported this viewpoint which evidenced by increased serum MDA and urinary excretion of 4HNE and 8-OHdG in db/db mice. Although artemether only presented slight inhibitory effect on fatty acid oxidation, the lipid peroxidation products were significantly reduced by artemether. The liver is an important place to produce ROS, and redox imbalance is implicated in the pathophysiological process of various liver diseases [21]. In the diabetic liver, the proteins related to redox homeostasis were significantly dysregulated. Artemether may restore redox homeostasis by

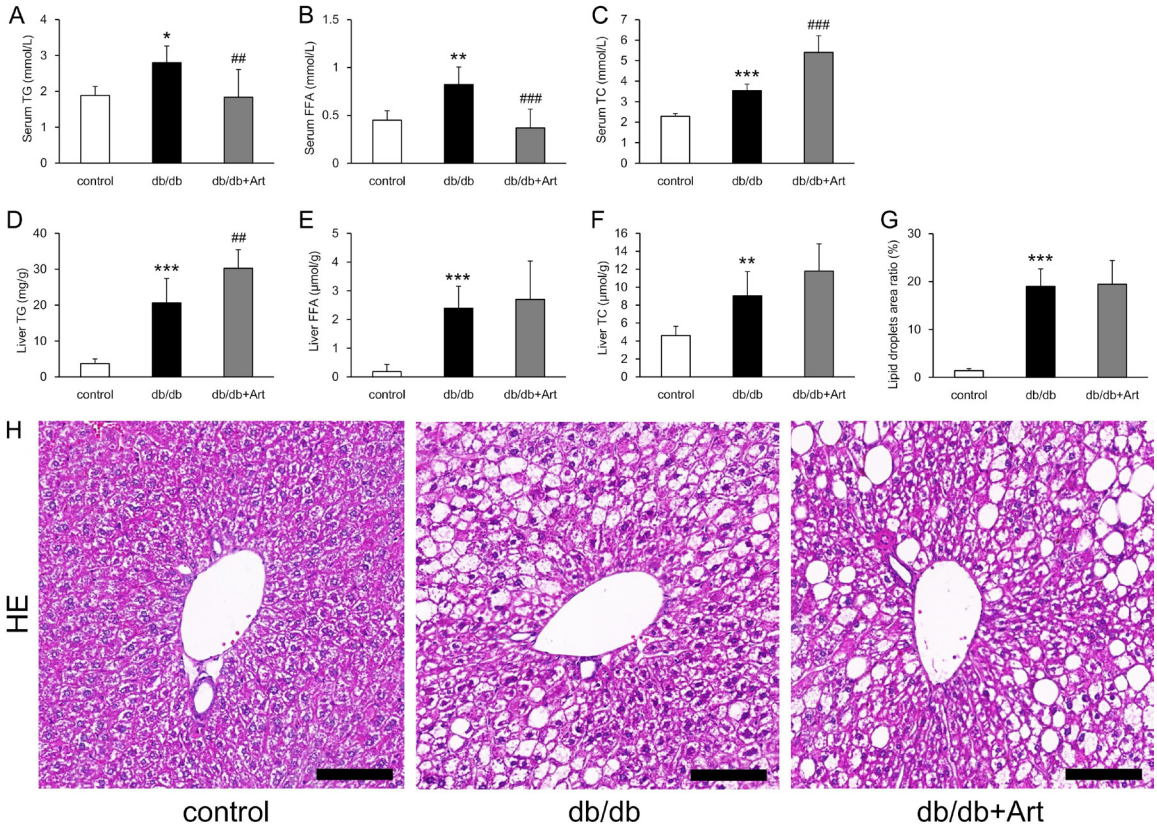

Figure 5. Effects of artemether on serum and liver lipid contents. A-C. The serum levels of TG, FFA, and TC in various groups. D-F. Bar graphs displayed the liver contents of TG, FFA, and TC in different groups. G. Bar graph showed the lipid droplets area ratio in each group under HE staining. n=6 per group. *P<0.05, **P<0.01 and ***P<0.001 vs. control group; $^{\#\#}$P<0.01 and $^{\#\#\#}$P<0.001 vs. the db/db group. H. Representative images of HE staining of liver sections from each group. Scale bar, 100 μm.

strengthening anti-lipid peroxidation ability through GPX4.

Compared to control group mice, an abnormally large and heavy liver was observed in diabetic db/db mice. According to the biochemical determinations and pathological staining of liver tissue, we speculate that the enlarged liver was mainly due to increased glycogen storage and lipid accumulation. Interestingly, both glycogen synthesis and degradation signals were significantly enhanced in the liver, which can be shown by obviously increased GS and PYGL. The overall trend is what is currently being observed, an increase in liver glycogen storage. The conventional view is that increased gluconeogenesis was a major contributor to hyperglycaemia and diabetes [22]. In this study, there were no significant differences of PCK1 and PCK2 between control and db/db group. Significantly reduced G6Pase protein level was detected in the diabetic liver. These results suggested that gluconeogenesis might be suppressed to some degree as a result of increased glycogen storage. Although artemether treatment did not change the liver weight, it markedly reduced the liver glycogen content. This effect may be related to its promotion on pyruvate oxidation and inhibition on glycogen synthesis.

IRS1 plays a key role in transmitting signals from the insulin and IGF-1 receptors to intracellular pathways [23]. Significantly decreased IRS1 and slight reduction of IRS2 in db/db mice suggested that the insulin and IGF-1 signaling was compromised in the diabetic liver. Serum insulin was significantly raised by artemether, but the IGF-1 level was not obviously changed. Meanwhile, significantly upregulated IRS1 expression in liver was detected after arte-

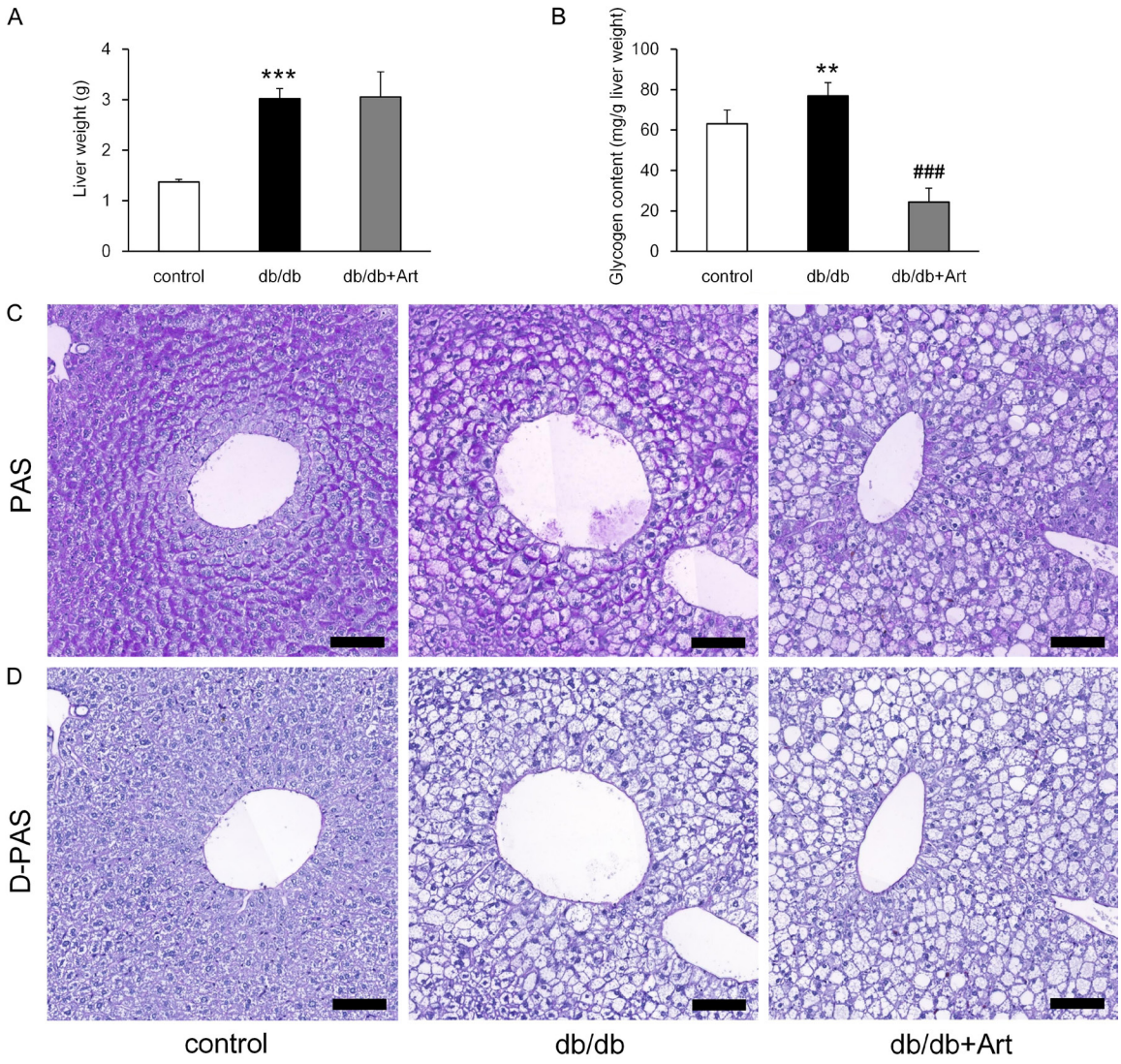

Figure 6. Effects of artemether on liver weight and glycogen content in db/db mice. (A, B) Bar graphs display the liver weight and glycogen content in different groups. n=6 per group. $^{**}P<0.01$ and $^{***}P<0.001$ vs. control group; $^{###}P<0.001$ vs. the db/db group. (C, D) Representative images of (C) PAS and (D) D-PAS staining of liver sections from each group (scale bar, 100 μm).

mether treatment. These results implied that the mechanism of artemether may be related to regulate insulin signaling pathway. The effect of artemether on insulin signal could reasonably explain the its promotion effect of lipid synthesis in liver. However, the elevation of serum insulin and the inhibition of liver glycogen synthesis are paradoxical after artemether intervention.

In summary, the present study demonstrated that artemether could regulate liver glycogen and lipid utilization in T2D mice, the underlying mechanisms were associated with its reinforcement on mitochondrial pyruvate oxidation in liver.

Acknowledgements

The present study was supported by the National Natural Science Foundation of China (82004156), the Shenzhen Science and Technology Project (JCYJ202205310924050-11; JCYJ20190812183603627) and the Shenzhen Fund for Guangdong Provincial High level Clinical Key Specialties.

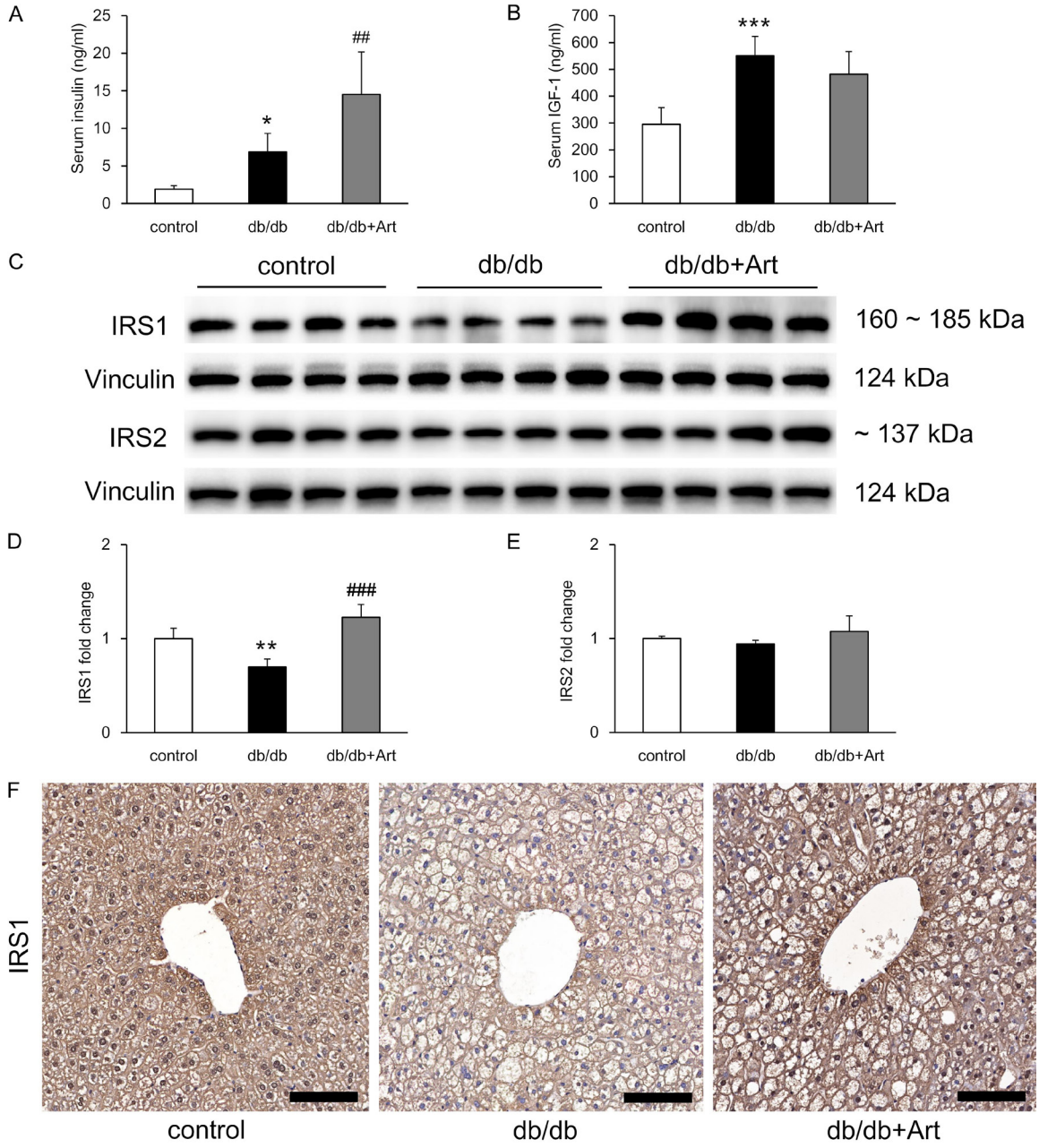

Figure 7. Artemether improved the insulin and IGF-1 associated signal transduction. A, B. The serum levels of insulin and IGF-1 in different groups. n=6 per group. C. Immunoblotting bands of IRS1 and IRS2 in various groups. D, E. Bar graphs displaying the fold changes of IRS1 and IRS2 in different groups. n=4 per group. *P<0.05, **P<0.01 and ***P<0.001 vs. control group; $^{\#\#}$P<0.01 and $^{\#\#\#}$P<0.001 vs. the db/db group. F. Representative immunohistochemical staining images of IRS1 from each group. Scale bar, 100 μm.

Disclosure of conflict of interest

None.

Address correspondence to: Huili Sun, Department of Nephrology, Shenzhen Traditional Chinese Medicine Hospital Affiliated to Nanjing University of Chinese Medicine, No. 1 Fuhua Road, Futian District, Shenzhen 518033, Guangdong, China. E-mail: sunhuili2011@126.com; shl1412@gzucm.edu.cn; Pengxun Han, Department of Nephrology, Shenzhen Traditional Chinese Medicine Hospital, The Fourth Clinical Medical College of Guangzhou University of Chinese Medicine, No. 1 Fuhua Road, Futian District, Shenzhen 518033, Guangdong, China. E-mail: hanpengxun@126.com; hpx2078@gzucm.edu.cn

References

[1] Roden M and Shulman GI. The integrative biology of type 2 diabetes. Nature 2019; 576: 51-60.

[2] Stefan N and Cusi K. A global view of the interplay between non-alcoholic fatty liver disease and diabetes. Lancet Diabetes Endocrinol 2022; 10: 284-296.

[3] Watt MJ, Miotto PM, De Nardo W and Montgomery MK. The liver as an endocrine organ-linking NAFLD and insulin resistance. Endocr Rev 2019; 40: 1367-1393.

[4] Zhang H, Ma J, Tang K and Huang B. Beyond energy storage: roles of glycogen metabolism in health and disease. FEBS J 2021; 288: 3772-3783.

[5] Geng Y, Faber KN, de Meijer VE, Blokzijl H and Moshage H. How does hepatic lipid accumulation lead to lipotoxicity in non-alcoholic fatty liver disease? Hepatol Int 2021; 15: 21-35.

[6] Gilbert M. Role of skeletal muscle lipids in the pathogenesis of insulin resistance of obesity and type 2 diabetes. J Diabetes Investig 2021; 12: 1934-1941.

[7] Choi HM, Kim HR, Kim EK, Byun YS, Won YS, Yoon WK, Kim HC, Kang JG and Nam KH. An age-dependent alteration of the respiratory exchange ratio in the db/db mouse. Lab Anim Res 2015; 31: 1-6.

[8] Weng W, Liu H, Sun Z, Zhou P, Yu X, Shao M, Han P and Sun H. Combined treatment with niclosamide ethanolamine and artemether combination improves type 1 diabetes via the targeting of liver mitochondria. Exp Ther Med 2022; 23: 239.

[9] Speijer D. Can all major ROS forming sites of the respiratory chain be activated by high FADH(2)/NADH ratios?: ancient evolutionary constraints determine mitochondrial ROS formation. Bioessays 2019; 41: e1800180.

[10] Speijer D. Molecular characteristics of the multi-functional FAO enzyme ACAD9 illustrate the importance of FADH(2)/NADH ratios for mitochondrial ROS formation. Bioessays 2022; 44: e2200056.

[11] Juan CA, Perez de la Lastra JM, Plou FJ and Perez-Lebena E. The chemistry of reactive oxygen species (ROS) revisited: outlining their role in biological macromolecules (DNA, lipids and proteins) and induced pathologies. Int J Mol Sci 2021; 22: 4642.

[12] Han P, Wang Y, Zhan H, Weng W, Yu X, Ge N, Wang W, Song G, Yi T, Li S, Shao M and Sun H. Artemether ameliorates type 2 diabetic kidney disease by increasing mitochondrial pyruvate carrier content in db/db mice. Am J Transl Res 2019; 11: 1389-1402.

[13] Cortassa S, Aon MA and Sollott SJ. Control and regulation of substrate selection in cytoplasmic and mitochondrial catabolic networks. A systems biology analysis. Front Physiol 2019; 10: 201.

[14] Smith RL, Soeters MR, Wust RCI and Houtkooper RH. Metabolic flexibility as an adaptation to energy resources and requirements in health and disease. Endocr Rev 2018; 39: 489-517.

[15] Ma N, Zhang Z, Liao F, Jiang T and Tu Y. The birth of artemisinin. Pharmacol Ther 2020; 216: 107658.

[16] Wang Y, Han P, Wang M, Weng W, Zhan H, Yu X, Yuan C, Shao M and Sun H. Artemether improves type 1 diabetic kidney disease by regulating mitochondrial function. Am J Transl Res 2019; 11: 3879-3889.

[17] Han P, Cai Y, Wang Y, Weng W, Chen Y, Wang M, Zhan H, Yu X, Wang T, Shao M and Sun H. Artemether ameliorates kidney injury by restoring redox imbalance and improving mitochondrial function in Adriamycin nephropathy in mice. Sci Rep 2021; 11: 1266.

[18] Wu T, Feng H, He M, Yue R and Wu S. Efficacy of artemisinin and its derivatives in animal models of type 2 diabetes mellitus: a systematic review and meta-analysis. Pharmacol Res 2022; 175: 105994.

[19] Price ER and Mager EM. Respiratory quotient: effects of fatty acid composition. J Exp Zool A Ecol Integr Physiol 2020; 333: 613-618.

[20] Morio B, Panthu B, Bassot A and Rieusset J. Role of mitochondria in liver metabolic health and diseases. Cell Calcium 2021; 94: 102336.

[21] Mooli RGR, Mukhi D and Ramakrishnan SK. Oxidative stress and redox signaling in the pathophysiology of liver diseases. Compr Physiol 2022; 12: 3167-3192.

[22] Shah AM and Wondisford FE. Tracking the carbons supplying gluconeogenesis. J Biol Chem 2020; 295: 14419-14429.

[23] Su J, Tang L, Luo Y, Xu J and Ouyang S. Research progress on drugs for diabetes based on insulin receptor/insulin receptor substrate. Biochem Pharmacol 2023; 217: 115830.